

ORIGINAL RESEARCH ARTICLE

# Characterization and assessment of potential microRNAs involved in phosphate-induced aortic calcification

Maya Fakhry<sup>1,2</sup> | Najwa Skafi<sup>1,2</sup> | Mohammad Fayyad-Kazan<sup>3</sup> |  
Firas Kobeissy<sup>4</sup> | Eva Hamade<sup>1</sup> | Saida Mebarek<sup>2</sup> | Aida Habib<sup>4,5</sup>  |  
Nada Borghol<sup>2</sup> | Asad Zeidan<sup>6,7</sup> | David Magne<sup>2</sup> | Hussein Fayyad-Kazan<sup>1</sup>  |  
Bassam Badran<sup>1</sup>

<sup>1</sup> Laboratory of Cancer Biology and Molecular Immunology, Faculty of Sciences I, Lebanese University, Hadath, Beirut, Lebanon

<sup>2</sup> Institute of Molecular and Supramolecular Chemistry and Biochemistry (ICBMS), UMR CNRS 5246, University of Lyon 1, Bâtiment Raulin, Villeurbanne Cedex, France

<sup>3</sup> Institut de Biologie et de Médecine Moléculaires, Université Libre de Bruxelles, Gosselies, Belgium

<sup>4</sup> Department of Biochemistry and Molecular Genetics, Faculty of Medicine, American University of Beirut, Beirut, Lebanon

<sup>5</sup> INSERM-U1149, CNRS-ERL8252, Centre de Recherche sur l'Inflammation, and the Sorbonne Paris Cité, Laboratoire d'Excellence Inflamex, Faculté de Médecine, Site Xavier Bichat, Université Paris Diderot, Paris, France

<sup>6</sup> Cardiovascular Physiology Lab, Department of Anatomy, Cell Biology and Physiology, Faculty of Medicine, American University of Beirut, Beirut, Lebanon

<sup>7</sup> College of Medicine, Qatar University, Doha, Qatar

## Correspondence

Eva Hamade, Laboratory of Cancer Biology and Molecular Immunology, Lebanese University, Faculty of Sciences I, Hadath, Beirut, Lebanon.

Email: eva.hamade@ul.edu.lb

Asad Zeidan, Department of Anatomy, Cell Biology and Physiological Sciences, American University of Beirut, Faculty of Medicine. DTS, PO BOX 11-0236, Beirut 1107-2020. Email: asad.zeidan@aub.edu.lb

## Funding information

Lebanese University and the Lebanese National Council for Scientific Research (CNRS), Grant number: 05-06-2014 (EH)

Medial artery calcification, a hallmark of type 2 diabetes mellitus and chronic kidney disease (CKD), is known as an independent risk factor for cardiovascular mortality and morbidity. Hyperphosphatemia associated with CKD is a strong stimulator of vascular calcification but the molecular mechanisms regulating this process remain not fully understood. We showed that calcification was induced after exposing Sprague-Dawley rat aortic explants to high inorganic phosphate level ( $P_i$ , 6 mM) as examined by Alizarin red and Von Kossa staining. This calcification was associated with high Tissue-Nonspecific Alkaline Phosphatase (TNAP) activity, vascular smooth muscle cells de-differentiation, manifested by downregulation of smooth muscle 22 alpha (SM22 $\alpha$ ) protein expression which was assessed by immunoblot analysis, immunofluorescence, and trans-differentiation into osteo-chondrocyte-like cells revealed by upregulation of Runt related transcription factor 2 (Runx2), TNAP, osteocalcin, and osteopontin mRNA levels which were determined by quantitative real-time PCR. To unravel the possible mechanism(s) involved in this process, microRNA (miR) expression profile, which was assessed using TLDA technique and thereafter confirmed by individual qRT-PCR, revealed differential expression 10 miRs, five at day 3 and 5 at day 6 post  $P_i$  treatment versus control untreated aortas. At day 3, miR-200c, -155, 322 were upregulated and miR-708 and 331 were downregulated. After 6 days of treatment, miR-328, -546, -301a were upregulated while miR-409 and miR-542 were downregulated. Our results indicate that high  $P_i$  levels trigger aortic calcification and modulation of certain miRs. These observations suggest that mechanisms regulating aortic calcification might involve miRs, which warrant further investigations in future studies.

## KEYWORDS

aorta, calcification, inorganic phosphate, microRNAs, trans-differentiation

## 1 | INTRODUCTION

Medial vascular calcification is a pathological process associated with chronic kidney disease (CKD) and type II diabetes mellitus (Sage, Tintut, & Demer, 2010; Zhu, Mackenzie, Farquharson, & Macrae, 2012). Cardiovascular mortality in CKD dialysis patients is 10–20 times higher than in the general population, and accounts for more than half of all deaths in CKD patients (Blacher, Guerin, Pannier, Marchais, & London, 2001; Foley, Parfrey, & Sarnak, 1998a, 1998b; Gansevoort et al., 2011; Schlieper et al., 2008; Sigrist, Taal, Bungay, & McIntyre, 2007). Virtually, all hemodialysis patients develop coronary artery calcification (Goodman et al., 2000) which is a strong predictor of coronary heart disease in patients with end-stage renal disease (ESRD, stage 5 CKD) (London et al., 2003). Clinically, the calcification of the medial layer mainly leads to an increase in arterial stiffness which can have an extremely detrimental effect, especially when considering large arteries, like the aorta (London et al., 2003). Normally, due to its elasticity, the aorta stores energy and blood during systole, and then releases it during diastole to the peripheral circulation as well as to the coronary artery thus providing a continuous blood flow and enabling left ventricular relaxation (Windkessel function of the aorta) (Belz, 1995). The loss of aortal elasticity and stiffness was reported to result in an increase in both systolic pressure and cardiac work which, in turn, can lead to heart failure, left ventricular hypertrophy along with diastolic dysfunction (Belz, 1995; Demer & Tintut, 2008).

Few therapeutical strategies have been proposed to attenuate vascular calcification in CKD patients, which includes phosphate binder, calcimimetic, and vitamin K2 administration (Stenvinkel, 2010). Among those, none has provided satisfying cardio-therapeutic outcomes thus highlighting the urgent need for efficient therapies especially that CKD reached epidemic proportions of 10–13% in some countries (Stenvinkel, 2010).

Mechanistically, arterial calcification is known to be an active process mediated by VSMCs, the predominant cell type in the medial layer of the artery wall (Belz, 1995; Doherty et al., 2004; Jono et al., 2000). Under pathological conditions, these cells are able to trans-differentiate into osteochondrocyte-like cells, with increased expression of osteoblast-chondrocytes markers including RUNX2, TNAP, osteocalcin, and osteopontin (Doherty et al., 2004). In fact, CKD is associated with numerous metabolic and endocrine disturbances, including inflammation coupled to abnormalities in calcium and phosphate metabolism, that contribute to this event (Lewis, 2012; Nitschke & Rutsch, 2012; Tintut, Patel, Parhami, & Demer, 2000). Hyperphosphatemia is prevalent in this disease and is caused mainly by hormonal imbalances (De Oliveira et al., 2013). Elevation in phosphate levels was described to induce medial calcification and VSMC osteogenic differentiation in different *in vitro*, *ex vivo*, and *in vivo* models (Chen et al., 2006; Giachelli, 2009; Jono et al., 2000; Larsson et al., 2010). Phosphate has been shown to promote calcification of human aortic smooth muscle cells in culture (Jono et al., 2000). In addition, different reports indicated that high phosphate induces medial VSMC calcification using an *ex vivo* rat aorta models (Giachelli, 2009; Larsson et al., 2010). Along the same line, high phosphate diet

was shown to induce medial calcification and accelerate VSMC osteogenic differentiation in an uremic mouse model of CKD (Chen et al., 2006). Altogether, these studies highlight a critical role for elevated phosphate levels in promoting osteo/chondrogenic differentiation of VSMCs in the medial layer of artery wall. However, the specific mechanism(s) responsible for these changes remain to be fully characterized.

Recently, an important role for microRNAs (miRs) during vascular calcification has been reported (Leopold, 2014). MiRs are short noncoding RNAs that regulate gene expression, at post-transcriptional level, upon binding to the 3'/5'-untranslated region (UTR) of their target messenger RNA (mRNA) and triggering either mRNA degradation or inhibition of translation (Erson & Petty, 2008). MiRs have been identified as important regulators in diverse differentiation processes including chondrogenesis and osteogenesis (Fakhry, Hamade, Badran, Buchet, & Magne, 2013; Hu et al., 2010). However, their contribution to these processes particularly in vascular calcification is not yet fully elucidated.

In this study, we first characterized a high phosphate model of vascular calcification after exposing rat aortic explants to high P<sub>i</sub> concentration (6 mM). Those aortas showed calcified phenotype associated with elevated expression of trans-differentiation markers (Runx2, TNAP, osteocalcin, and osteopontin) compared to control untreated aortas. Next, we characterized the miR expression profile in high P<sub>i</sub>-treated aorta versus control samples and showed a significant alteration of different miRs suggesting their potential importance in regulating the early inflammatory response and calcification and trans-differentiation events mediated by hyperphosphatemia.

## 2 | MATERIALS AND METHODS

### 2.1 | Animal study

All procedures were in accordance with the National Institutes of Health Guide for the Care and Use of Laboratory Animals. The basic principles governing animal research were approved by the Animal Ethics Committee, American University of Beirut (IACUC # 12-08-235).

### 2.2 | Aorta tissue harvest

Male Sprague-Dawley rats (200–250 g) were euthanized by CO<sub>2</sub> inhalation. Under aseptic conditions, aorta was cut from its posterior till its anterior end, was cleaned, infused by phosphate-buffered saline (PBS) buffer (37°C) and adventitia layer was removed by gentle scraping of external part.

### 2.3 | Aorta organ culture

Tissues were cultured in Dulbecco's Modified Eagle's Medium (DMEM, Sigma), (4.5 g/L glucose) supplemented with 10% fetal bovine serum (FBS, Sigma), penicillin (100 U/ml), streptomycin (100 µg/ml), 20 mmol/L HEPES, and 2 mmol/L L-glutamine. Tissues were maintained at 37°C in a humidified atmosphere with 5% CO<sub>2</sub> in air.

Treatment involved the addition of 5 mM inorganic phosphate ( $P_i$ ) into DMEM medium that contains initially 1 mM  $P_i$  to reach a final concentration of 6 mM  $P_i$ . For tissue sectioning, the collected aortas were snap-frozen in liquid nitrogen and stored at  $-80^\circ\text{C}$  and processed according to standard procedures. Tissue sections ( $4\ \mu\text{m}$ ) were performed from the small part of the aortic arch

## 2.4 | RNA extraction, reverse transcription, and quantitative PCR (qRT-PCR)

Total RNA was extracted using TriPure isolation reagent (Sigma-Aldrich, St Louis, MO) according to the manufacturer's instructions. Integrity of RNA was checked by running a gel electrophoresis and  $1\ \mu\text{g}$  of each RNA sample was used for reverse transcription performed using iScript reverse transcription kit (Bio-Rad, Hercules, CA). The reaction was carried out at  $25^\circ\text{C}$  for 5 min,  $42^\circ\text{C}$  for 30 min and stopped with incubation at  $85^\circ\text{C}$  for 5 min. Quantitative PCR was performed using iQ SYBR Green Supermix (Bio-Rad) and a CFX96 PCR detection system (Bio-Rad). The cycling conditions began by  $95.0^\circ\text{C}$  for 10 min, 40 cycles of  $95.0^\circ\text{C}$  for 30 s,  $57.0^\circ\text{C}$  for 30 s,  $72.0^\circ\text{C}$  for 1 min, and a final extension at  $72.0^\circ\text{C}$  for 8 min. Relative quantification analysis was performed using the Livak method ( $2^{-\Delta\Delta C_t}$ ). GAPDH (glyceraldehyde-3-phosphate dehydrogenase) gene was used as a reference gene. The sequence of the primers is indicated in the Table 1 of the supplement section and was synthesized by Sigma-Aldrich.

## 2.5 | TNAP activity measurement

Crushed aortas were lysed in 0.2% Nonidet-P40 followed by 30 s of sonication, centrifugation for 5 min at  $4,000\times g$ , and collection of the supernatants. TNAP activity was assessed using paranitrophenylphosphate (pNPP) (Lancaster Synthesis, Ward Hill, MA) as substrate. Absorbance of yellow dephosphorylated product was measured with spectrophotometer at 405 nm after sample-reactive incubation at  $37^\circ\text{C}$  for 30 min. The activity was calculated and normalized to the protein concentration.

## 2.6 | Alizarin red staining (AR-S)

Intact aortas were fixed with ethanol 95% for 24 hr, stained with Alizarin red (Sigma-Aldrich) 0.003% in 1% potassium hydroxide (KOH) for 30 hr, and washed twice with 2% KOH. Images were captured with normal camera.

## 2.7 | Von Kossa staining

Intact aortas were fixed with 70% ethanol at room temperature and washed with autoclaved water. This was followed by incubation in 5% silver nitrate for 30 min and washes with autoclaved water. The tissues were thereafter incubated for 1 hr under UV light, washed twice in 5% sodium thiosulfate and counter stained with 0.1% eosin dye. After washing and dryness, images were captured with a normal camera.

## 2.8 | Immunoblot analysis

Proteins were extracted from crushed aortas using Laemmli buffer with 5% protease inhibitor (Roche). After centrifugation at  $8,000\times g$ , supernatants were collected and heated at  $95^\circ\text{C}$  for 5 min. Protein concentration was determined by Lowry method (Bio-Rad). A 5%  $\beta$ -mercaptoethanol was added to the samples. Thirty microgram of proteins were separated by 12% SDS-PAGE and transferred to nitrocellulose membranes which were next blocked by 5% non-fat milk and further incubated with a rabbit polyclonal antibody anti-SM22 alpha (Abcam, ab155272) (1:1,000). The immune complexes were detected using Clarity ECL Western blotting substrate (Bio-Rad) and were revealed with the high-resolution ChemiDoc MP system (Bio-Rad). Membranes were washed in "stripping buffer" and further incubated with a mouse antibody anti-GAPDH (Cruz Biotechnology, Santa Cruz, CA) (1:1,000). Band intensity was quantified using ImageJ software.

## 2.9 | SM22 $\alpha$ immunofluorescence

Tissue sections on slides were washed twice with PBS buffer containing 1% Triton X-100, incubated in blocking solution for 1 hr at room temperature (normal goat serum 10%, bovine serum albumin 3%), washed twice with the same buffer, and incubated overnight at  $4^\circ\text{C}$  with the primary antibody rabbit anti-SM22 alpha antibody (cat # ab155272, 1/1000 dilution, Abcam, Cambridge, UK). This was followed by two washes with the same buffer and then incubation with secondary anti-rabbit antibody conjugated to Alexa Fluor 488 (Abcam, ab150077) (RRID: AB\_2630356) (1/1000) for 1 hr at room temperature. Three washes with the same buffer were performed prior to incubation with Hoechst solution for 10 min followed by three washes with the same buffer. Slides were mounted with Fluoromount Aqueous Mounting Medium (Sigma-Aldrich) mixed with Prolong Gold

**TABLE 1** Summary of primers used in qRT-PCR

Gene	Forward primer 5' → 3'	Reverse primer 5' → 3'
<i>rGapdh</i>	GGCACAGTCAAGGCTGAGAATG	ATGGTGGTGAAGACGCCAGTA
<i>rRunx2</i>	GCCGGGAATGATGAGAATA	TTGGGGAGGATTGTGAAGA
<i>rOcn</i>	GGTGCAGACCTAGCAGACACCA	AAGTAGCGCCGAGTCTATTCA
<i>rTnap</i>	AACGTGGCCAAGAATCATCA	TGTCCATCTCCAGCCGTGTC
<i>rOpn</i>	GATCGATAGTGCCGAGAAGC	TGAGGTGATGTCCTCGTCTG

antifade reagent (Thermo Fisher Scientific, Waltham, MA). Pictures were taken using Zeiss Axio fluorescence microscope with ZEN software (<https://www.zeiss.com>, RRID: SCR\_013672) and fluorescence intensity was quantified using image J software (four pictures per aorta/ three aortas).

## 2.10 | TaqMan Low Density Array (TLDA)

A two-step procedure was performed to profile the miRNAs. First, for cDNA synthesis from the miRNAs, 100 ng of total RNA from control and treated aortas was subjected to reverse transcription (RT) using a TaqMan® microRNA reverse transcription kit and Megaplex RT primers (Thermo Fisher Scientific) according to the manufacturer's protocol, allowing simultaneous reverse transcription of 380 mature rat miRNAs. RT was performed on a Mastercycler Egradient thermocycler (VWR International, Leuven, Belgium) with the following cycling conditions: 40 cycles of 16°C for 2 min, 42°C for 1 min, and 50°C for 1 s, followed by a final step of 80°C for 5 min to inactivate the reverse transcriptase.

After the amplification step, the products were diluted with RNase-free water, combined with TaqMan gene expression master mix, and then loaded into TaqMan rat MicroRNA array (Thermo Fisher Scientific), which is a 384-well formatted plate and real-time PCR-based microfluidic card with embedded TaqMan primers and probes in each well for the 380 different mature rat miRNAs; the U87 transcript was used as a normalization signal. Quantitative PCR was performed according to the manufacturer's instructions. Quantitative PCR was performed on an ABI PRISM 7900HT sequence detection system (Thermo Fisher Scientific) with the following cycling conditions: 50°C for 2 min and 94.5°C for 10 min followed by 40 cycles of 95°C for 30 s and 59.7°C for 1 min. The cycle threshold ( $C_q$ ) was automatically given by SDS 2.3 software (Thermo Fisher Scientific) and is defined as the fractional cycle number at which the fluorescence passes the fixed threshold of 0.2. U87 embedded in the TaqMan rat microRNA arrays was used as an endogenous control. The relative expression levels of miRNAs were calculated using the comparative  $\Delta\Delta C_q$  method. The -fold changes in miRNAs were calculated by the expression  $2^{-\Delta\Delta C_q}$ .

## 2.11 | Taqman miRNA Assay for Individual miRNAs

Gene-specific reverse transcription was performed for each miR using 10 ng of purified total RNA, 100 mM dNTPs, 50 units of MultiScribe reverse transcriptase, 20 units of RNase inhibitor, and 50 nM gene-specific RT primer samples using the TaqMan microRNA reverse transcription kit (Thermo Fisher Scientific). A 15- $\mu$ l reactions were incubated for 30 min at 16°C, 30 min at 42°C, and 5 min at 85°C to inactivate the reverse transcriptase. Quantitative PCRs (5  $\mu$ l of RT product, 10  $\mu$ l of TaqMan 2 $\times$  universal PCR master mix (Thermo Fisher Scientific), and 1  $\mu$ l of TaqMan microRNA assay mix containing PCR primers and TaqMan probes) were carried out on an ABI Prism 7900HT sequence detection system (Thermo Fisher Scientific) at 95°C for 10 min followed by 40 cycles at 95°C for 15 s and 60°C for 1 min. All

quantitative PCRs were performed in triplicate. The expression levels ( $2^{-\Delta\Delta C_q}$ ) of miRNAs were calculated.

## 2.12 | MicroRNAs-gene interaction analysis

The identified miRs were analyzed using the Elsevier's Pathway Studio software package version 10.0 (Ariadne Genomics/Elsevier) (<http://www.elsevier.com/solutions/pathway-studio-biological-research>; RRID: SCR\_014979) to construct the downstream target genes using its proprietary molecular interaction database namely ResNet 9.0. We utilized direct interaction, downstream regulators as well as "Subnetwork Enrichment Analysis" (SNEA) algorithm to extract statistically significant altered biological processes pertaining to each identified set of regulated microRNAs. SNEA utilizes Fisher's statistical test to determine if there are non-randomized associations between two categorical variables organized by specific relationship.

## 2.13 | Statistical analysis

Experiments were performed in triplicates and repeated for three independent experiments. Results were expressed as mean  $\pm$  the standard error of the mean (SEM). For statistical analysis, a two-tailed unpaired Student *t*-test was performed (InStat program, version 3.1, Graphpad, La Jolla, CA) (Results were considered significant \* when  $p < 0.05$ , \*\* when  $p < 0.01$ , and \*\*\* when  $p < 0.001$ ).

# 3 | RESULTS

## 3.1 | High phosphate induces calcification of rat aortic explants

In order to determine the effect of high phosphate on the calcification ability of aortic explants, calcium deposition was assessed by alizarin red and Von Kossa staining methods following incubation of the rat aortic explants with  $P_i$  (6 mM) for 6 days. Alizarin red staining revealed high calcification level, visualized as small alizarin red precipitates, in treated aortas compared to untreated controls (Figure 1a). Consistent with these results, Von Kossa staining revealed the presence of dark gray calcium deposits in high  $P_i$ -treated explants but not in control (Figure 1b).

## 3.2 | High phosphate induces TNAP activity

Since VSMCs calcification largely relies on TNAP activity (Narisawa et al., 2007), we therefore examined the effect of  $P_i$  treatment. Figure 2 showed the TNAP activity in the explants the explants of 6 day treatment with high  $P_i$  concentration which exhibited a significant increase in TNAP specific activity compared to control untreated explants.

## 3.3 | High phosphate induces de-differentiation of aortic VSMCs

To determine whether phosphate treatment induces de-differentiation of VSMCs in the aortic explants, we next investigated the expression

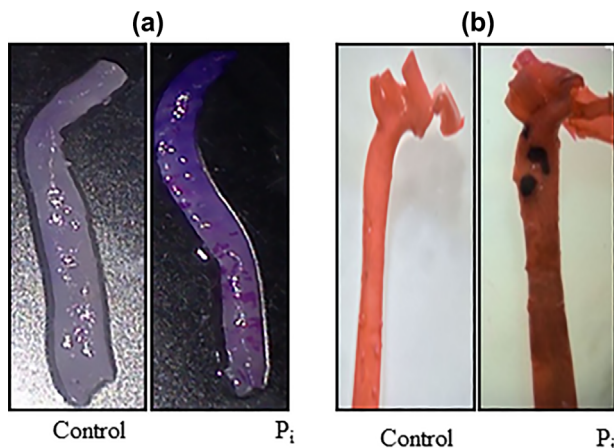


**FIGURE 1** Calcification of aortic explants is induced by high phosphate. (a) Alizarin red and (b) Von Kossa staining of intact aorta tissues. Calcium deposition was observed after 6 days of culture with high phosphate ( $P_i$ ) medium compared with culture with control medium

level of the smooth muscle-specific protein SM22 $\alpha$  in high  $P_i$ -treated versus untreated aortic explants by immunoblot analysis (control). As shown by immunoblot (Figure 3a) and densitometric analysis of SM22 $\alpha$  (Figure 3b), explants incubated with high  $P_i$  for 6 day exhibited significant downregulation of SM22 $\alpha$  protein level. To further confirm this observation, we assessed SM22 $\alpha$  expression by immunofluorescence and showed that similar treatment of explants significantly attenuated the fluorescence intensity (Figures 3c and 3d). These data indicate that VSMCs de-differentiation is induced in response to high  $P_i$ .

### 3.4 | High phosphate induces aortic VSMCs trans-differentiation into osteo-chondrocyte like cells

To determine whether VSMCs in the rat aortic explants are capable to trans-differentiate into osteo-chondrocyte like cells in the presence of high  $P_i$  concentration (6 mM), the mRNA levels of different

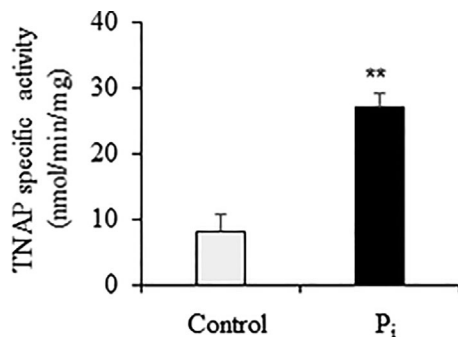


**FIGURE 2** TNAP activity is induced by high phosphate. TNAP activity was determined and normalized with specific protein concentration. A significant increase in TNAP specific activity was observed after 6 days of culture in high phosphate ( $P_i$ ) medium compared to control medium. Results represent the mean  $\pm$  SEM of three independent experiments, \*\* indicates  $p$  value  $<0.01$

osteoblastic or chondrogenic differentiation markers were assessed using qRT-PCR.

Interestingly, phosphate treatment for 6 days induced a significant increase in the transcription level of Runx2, the transcription factor that is necessary for the differentiation of osteoblasts and hypertrophic chondrocytes (Figure 4a). In addition, the mRNA levels of other osteo-chondrocyte differentiation markers like *Tnap* and *Osteopontin* (*Opn*) were significantly elevated following  $P_i$  treatment starting from 3 days treatment (Figures 4b and 4c) and 6 days for *Osteocalcin* (*Ocn*) (Figure 4d).

Finally, the mRNA expression level of collagen type II, indicative of an early stage in chondrocyte differentiation, was not altered after  $P_i$  treatment for 6 days (data not shown). Altogether, these data indicate that phosphate triggers the trans-differentiation of VSMCs in the aortic explants into osteoblast/chondrocyte-like cells.

### 3.5 | High phosphate induces an alteration in the microRNA expression profile of aortic explants

To unravel the possible mechanism(s) by which calcification and trans-differentiation were mediated in response to high phosphate, we hypothesized that microRNAs might be involved in regulating this process. TLDA technique was applied to characterize the miR expression profile in high  $P_i$ -treated versus untreated aortas. TLDA analysis revealed 17 differentially expressed and statistically significant miRs after 3 days of  $P_i$  treatment compared to untreated controls. These miRs include: miR-107, -133b, -135a, -223, -323, -331, -598, -708, -155, -186, -200c, -296, -322, -345, -375, -491, -582. Among those miRs, five were confirmed to have a significant differential expression by individual qPCR assays. Three miRs were upregulated (miR-155, -200c, -322) whereas two miRs were downregulated (miR-331, -708) in treated aortas (Figure 5). At day 6, TLDA analysis revealed 16 statistically significant differentially expressed miRs (miR-188-5p, -197, -215, -219, -291a, -335, -409, -499, -542, -672, -224, -301a, -31, -328, -546, -590) among which only five miRs (miR-328, -546, -301a, -409, and -542) were confirmed by individual qRT-PCR to be differentially expressed (Figure 5b). In fact, miR-328, -546, and -301a showed upregulated expression whereas miR-409 and -542 were downregulated in  $P_i$ -treated aortas compared (Figure 5). These data indicate a possible involvement of these miRs in regulating aortic calcification and the expression of the osteoblast-chondrocyte differentiation markers in response to phosphate treatment.

### 3.6 | Potential genes found to be targeted by the differentially expressed microRNAs

To further determine how these differentially expressed miRs can contribute to the process of aortic calcification, we have investigated their downstream regulated target genes using the Elsevier's Pathway Studio software package. Several genes were found to be targets for the differentially expressed miRs at day 6 (Figure 6). In the set of upregulated miRs, miR-328 was found to have 12 target genes including calcineurin while miR-301a showed 10 targets among which

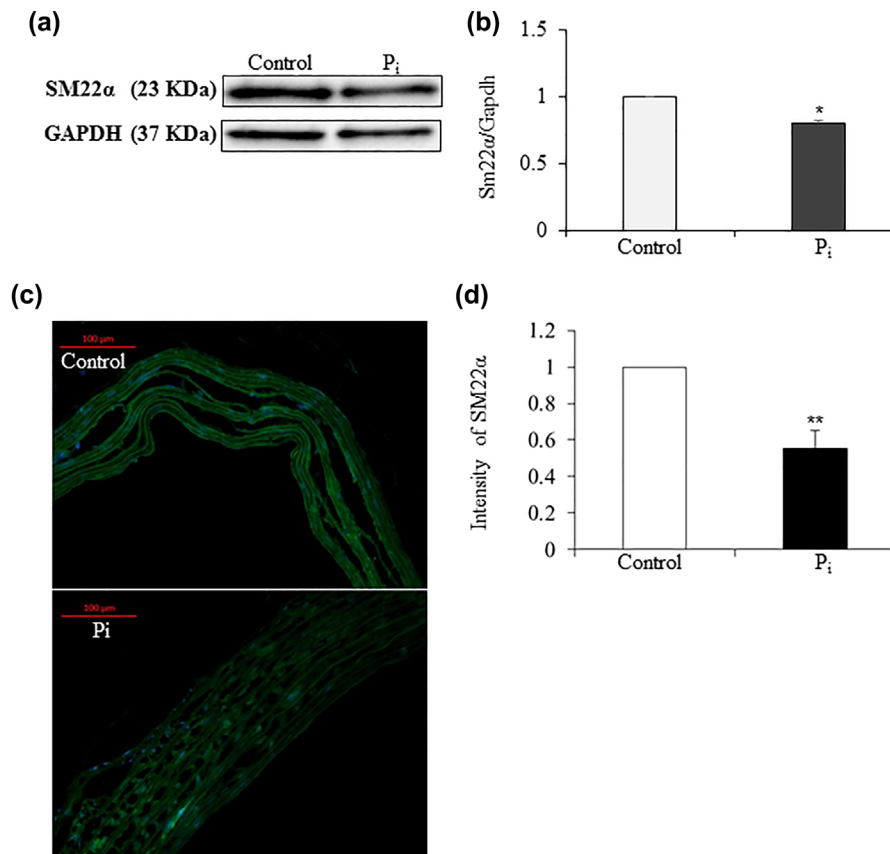


**FIGURE 3** De-differentiation of aortic cells is induced by high phosphate. (a) Shows Western blot analysis of SM22 $\alpha$  and GAPDH and (b) the densitometric analysis of SM22 $\alpha$  corrected to GAPDH expression. Each value represents the mean  $\pm$  SEM of three independent experiments. \* indicates a statistical significance with  $p < 0.05$ . (c) shows the SM22 $\alpha$  examined by Immunofluorescence on tissue sections and (d) quantification analysis of the immunofluorescence of SM22 $\alpha$ . A significant downregulation of SM22 $\alpha$  protein level was observed after 6 days of culture in high phosphate (P<sub>i</sub>) medium compared to control medium. For the Immunofluorescence, the value represents the mean  $\pm$  SEM of four independent experiments. \*\* indicates a statistical significance with  $p < 0.01$

are inflammatory cytokines, Nuclear Factor kappa-light-chain-enhancer of activated B cells (NF- $\kappa$ B), and mitogen-activated protein kinase 3 (MAPK3). In the set of downregulated miRs, miR-409 was found to target matrix metalloproteinase2, 9 (MMP2, MMP9), fibrinogen, caspase 3 (CASP3) and UL16 binding protein 1 (ULBP1), while miR-542 was found to have matrix metalloproteinases, albumin (ALB), matrix metalloproteinase3 (MMP3), TNF receptor-associated factor 4 (TRAF4) and RNA-induced silencing complex (RISC) complex as targets. These results highlight several important networks of pathways and functions to be associated with the targeted genes, which in turn may contribute to the previously observed phenotypic changes of aortic explants in response to P<sub>i</sub>.

## 4 | DISCUSSION

VSMCs trans-differentiation into osteoblast/chondrocyte-like cells plays a crucial role in promoting arterial calcification (Belz, 1995; Doherty et al., 2004; Jono et al., 2000). Among the multiple factors that might be involved, phosphate level is considered to be crucial

(Chen et al., 2006; Giachelli, 2009; Jono et al., 2000; Larsson et al., 2010). Using a rodent ex vivo high phosphate model that mimics hyperphosphatemia-induced arterial calcification observed in CKD, we demonstrated that P<sub>i</sub> treated aortic explants were capable to mineralize, in association with an increased TNAP activity. Although vascular calcification cause in CKD is multifactorial, it may rely largely on TNAP. In fact, TNAP hydrolyses the mineralization inhibitor, inorganic pyrophosphate (PP<sub>i</sub>) which is produced locally by VSMCs and is provided systematically by the liver (Jansen et al., 2014, p. 6). PP<sub>i</sub> acts as a constitutive mineralization inhibitor whose mere removal is sufficient to induce calcification of the media of the artery wall (Rutsch et al., 2001; Sheen et al., 2015). Furthermore, aortas in culture release PP<sub>i</sub> and their calcification in the presence of high phosphate and calcium concentrations proceeds only when PP<sub>i</sub> is removed by TNAP (Lomashvili, Cobbs, Hennigar, Hardcastle, & O'Neill, 2004) which is known to have high activity in VSMCs of uremic animals' aortas (Lomashvili, Garg, Narisawa, Millan, & O'Neill, 2008).

In fact, inflammation is likely one of the factors able to induce TNAP in VSMCs where tumor necrosis factor alpha (TNF- $\alpha$ ) for instance was shown to induce TNAP expression in VSMCs and trigger

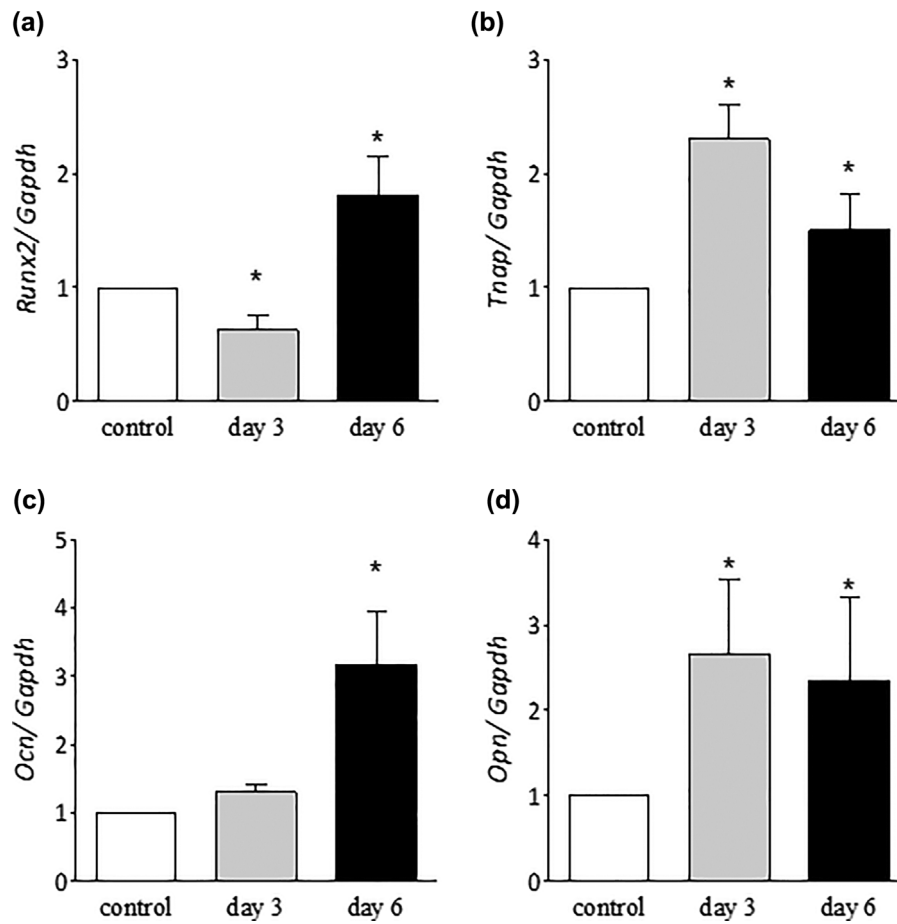


**FIGURE 4** Trans-differentiation of aortic cells into osteo-chondrocyte like cells is induced by high phosphate. Aortic explants were cultured for 3 and 6 days under control or high phosphate ( $P_i$ ) and the mRNA level of different markers, *Runx2* (a), *Tnap* (b), *Ocn* (c), and *Opn* (d), was assessed by qRT-PCR. Each value represents the mean  $\pm$  SEM of three independent experiments. \* indicates a statistical significance with  $p < 0.05$

VSMC trans-differentiation into osteoblast/chondrocyte-like cells (Bessueille & Magne, 2015; Masuda, Miyazaki-Anzai, Levi, Ting, & Miyazaki, 2013; Tintut et al., 2000; Zhao et al., 2012). TNAP is tissue-nonspecific, and its expression is induced by TNF- $\alpha$  independently of osteoblast or chondrocyte differentiation (Ding et al., 2009; Lencel et al., 2011). Inflammation is known to play an important role in promoting vascular calcification, in particular in the context of diabetes (Bessueille, Cell Mol Life Sci 2015). In the context of CKD, it is likely that the associated hyperphosphatemia is a more potent stimulator of calcification than inflammation. Moreover, in the present study, we aimed at characterizing the miRNAs associated with trans-differentiation and calcification and treating aortas with inflammatory cytokines would probably have modulated the expression of many miRNAs involved in inflammation but not directly linked to calcification. In this study, we also showed that phosphate stimulated de-differentiation and osteo-chondrocyte-like trans-differentiation in aortic cells as evidenced by a lower expression of the VSMCs differentiation marker SM22 $\alpha$  and a higher expression of osteo-chondrocyte trans-differentiation markers including Runx2, TNAP, OCN, and OPN in  $P_i$  treated versus control untreated aortic cells. These results are expected and coherent with earlier reports

demonstrating the calcification and trans-differentiation inductive roles of  $P_i$  on VSMCs (Chen et al., 2006; Giachelli, 2009; Jono et al., 2000; Larsson et al., 2010). Indeed, this is particularly relevant in patients with CKD where it is generally observed that CKD VSMCs differentiate toward osteoblasts in the medial layer (Vattikuti & Towler, 2004). These observations might have been extended with primary culture of extracted VSMCs but in this study we only focused on organ culture which is more similar to physiological conditions. This work proves again medial artery calcification as an actively regulated process. However, the precise mechanism and the specific pathways by which phosphate mediates aortic calcification and trans-differentiation are not well understood.

Recently, microRNAs were importantly recognized as crucial regulators of many cellular functions including differentiation, proliferation, migration, and apoptosis (Rana, 2007). These small noncoding RNA molecules often induce the mRNA degradation or the translational inhibition of several target genes (Guo, Ingolia, Weissman, & Bartel, 2010; Huntzinger & Izaurralde, 2011). A series of these microRNAs were shown to regulate physiological osteoblast differentiation, a key step in bone formation and mineralization (Fakhry et al., 2013; Hu et al., 2010). In addition, several other microRNAs were also

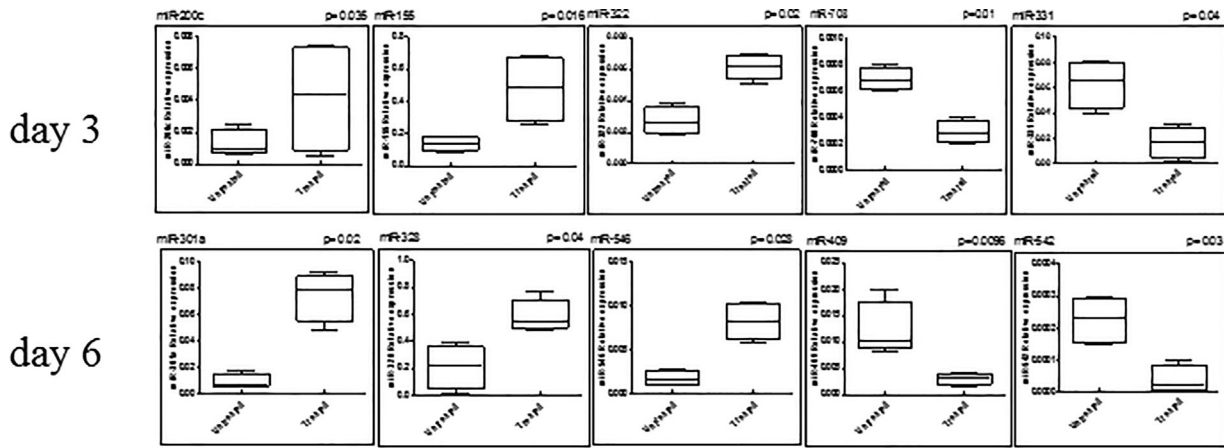


**FIGURE 5** MicroRNAs differential expression profile in Pi treated aortas. miRs were significantly differentially expressed between untreated control and high-phosphate treated aortas for 3 or 6 days from three independent experiments. Data obtained by qRT-PCR amplification of miRs were plotted. *p*-values for each miRNA are shown

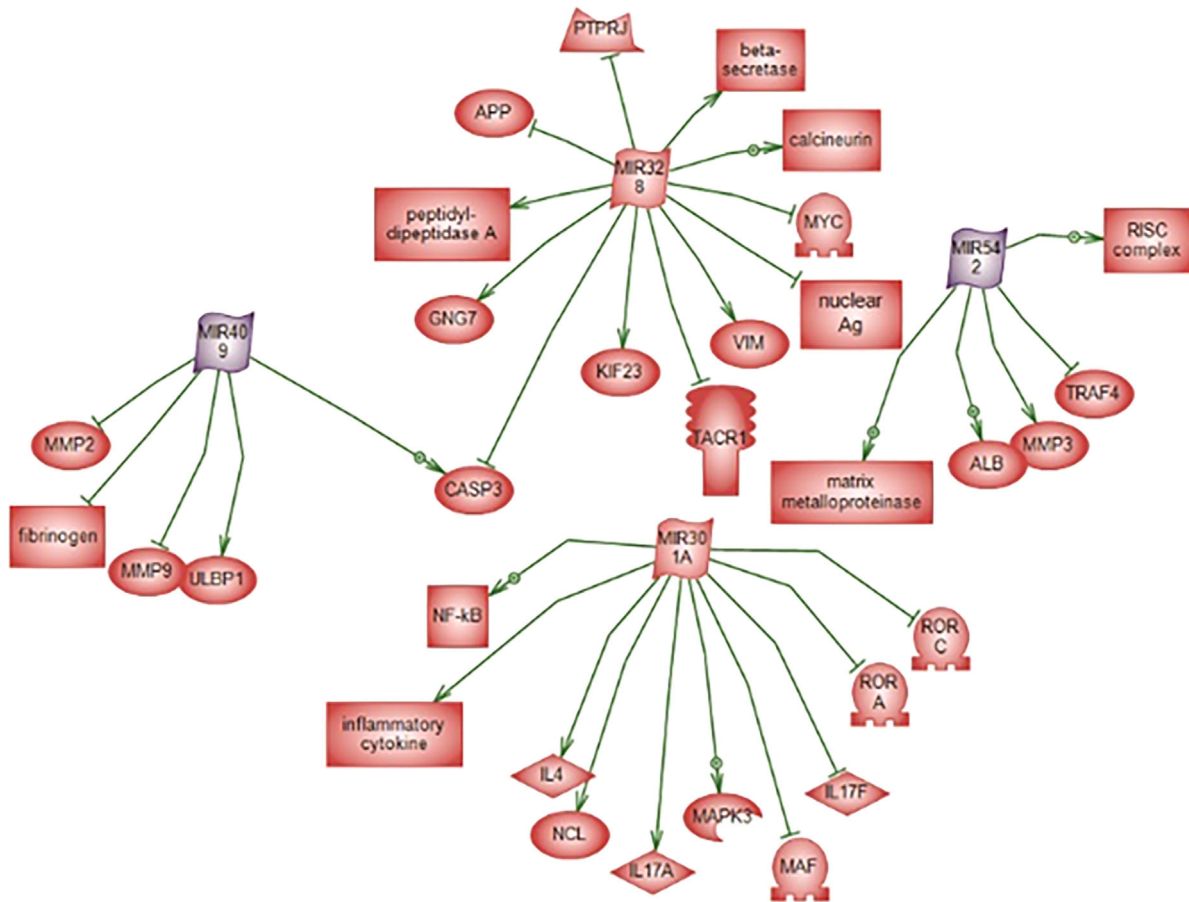


**FIGURE 6** Dysregulated miRNAs target genes as determined from MicroRNA-Gene Regulatory Network. Shown are the target genes for the dysregulated miRNAs. IR, microRNA; MAF, avian musculoaponeurotic fibrosarcoma oncogene homolog; MYC, mvelocytomatosis viral oncogene homolog (avian); RORA C, RAR-related orphan receptor AC; PTPRJ, protein tyrosine phosphatase, receptor type, J; ALB, albumin; XCL, nucleolin; KIF23, kinesin family member 23; VIM, vimentin; APP, amyloid beta (A4) precursor protein; IL4/17A/17F, interleukin 4/17A/17F; MAPK3, mitogen-activated protein kinase 3; CASP3, caspase 3, apoptosis-related cysteine peptidase; GXG7, guanine nucleotide binding protein (G protein), gamma 7; TACR1, tachykinin receptor 1; MMP2 3 9, matrix metalloproteinase2'3'9; ULBP1, UL16 binding protein 1; TRAF4, TXF receptor-associated factor 4; XF-kB, nuclear factor kappa-light-chain-enhancer of activated B cells; RISC, RXA-induced silencing complex

shown to likely modulate trans-differentiation of VSMCs and vascular calcification (Cui et al., 2012; Goettsch, Rauner, Pacyna, et al., 2011; Gross, Six, Kamel, & Massy, 2014; Panizo et al., 2015). In this study, we questioned whether a specific microRNA network is implicated in triggering rat artery calcification in response to  $P_i$  treatment.

In fact, our study pinpoints the possible involvement of microRNAs in regulating VSMC trans-differentiation and calcification in response to  $P_i$ , as we have speculated. This was revealed upon miR profiling which identified an altered miR expression level of five miRs (miR-155, -200c, -322, -331, and miR-708) 3 days post  $P_i$  treatment and five miRs (miR-328, -546, -301a, -409, and miR-542) 6 days post  $P_i$  treatment. This finding may suggest the presence of a network of targets regulated by these miRs leading to the onset of calcification. It is likely that miRs can regulate phenotype changes via distinctive microRNA programs with temporal and cell-specific signatures that initiate SMC calcification (Leopold, 2014). Importantly, we found different miR profiles between different days of culture. This is interesting because the process of vascular calcification involves many different steps starting with the initial trans-differentiation of smooth muscle cells under the effect of high phosphate the subsequent inflammation, oxidative stress and the increase in TNAP expression and activity, reaching the steps of osteoblasts or chondrocytes maturation before the steps of calcium deposition. At day 3, the cells were not showing a phenotype of mature osteo-chondrocytes when the osteocalcin expression was not changed, thus we were still in the steps of initial trans-differentiation. At day 6, we had a significant increase in osteocalcin gene expression, marking the presence of mature osteo-chondrocytes, which can directly calcify the extracellular matrix. These different processes in the two tested times are the bases of the change in the miR profile.

Among the miRs overexpressed in day 3, miR-155 and miR-200c have practical roles in inflammation in VSMCs. The overexpression of miR-155 in VSMCs isolated from rat thoracic aorta was shown to increase inflammation as seen by an NF- $\kappa$ B activation and oxidative stress as seen by p47<sup>phox</sup>. In this model the effects of miR-155 was mediated by ERK1/2 activation. Importantly, the overexpression of this miR also induced a decrease in SM22 $\alpha$  expression, which was shown also to be downregulated in our model (Yang et al., 2015). MiR-200 family was also shown to induce inflammation in VSMCs isolated from mouse thoracic aorta through inducing the expression of COX2, and it was found to be overexpressed in VSMCs isolated from diabetic mice, which is also a risk factor for vascular calcification (Reddy et al., 2012). In contrast, in another study involving preosteoblasts and bone marrow mesenchymal stem cells, miR-200c was shown to decrease inflammation by targeting IL-6 and IL-8. However, in this study the overexpression of miR-200c enhanced the osteogenic differentiation as evidenced by increased osteocalcin expression, as seen in our model (Hong et al., 2016). Thus, in our model it may be helping the osteogenic differentiation, but its role in inflammation must be assessed. MiR-322 was also upregulated in our model. Its overexpression in C2C12 myoblasts induces osteoblastic differentiation marked by an increase in the osteoblast transcription factors: Osterix and Runx2, and in osteocalcin. Also, it enhanced the

osteogenesis induced by BMP in this cell type. Thus, in our model this miR also may be responsible of the later increase in *Ocn* and *Runx2* gene expression (Gámez, Rodríguez-Carballo, Bartrons, Rosa, & Ventura, 2013). MiR-331, which was downregulated in our model at day 3, was shown to be anti-inflammatory in human airway epithelial Beas-2B cells, where its overexpression inhibits the activation of NF- $\kappa$ B and the expression of IL-6 and IL-8 in response to particulate matter (Song et al., 2017). Also, miR-708, which was also downregulated in our model, was proven to have anti-inflammatory roles in endothelial cells isolated from human aorta by inhibiting NF- $\kappa$ B signaling (Chen et al., 2015).

The interaction analysis performed helped to unravel the molecular pathways that are most likely to be involved. Some of these pathways are probably linked to artery calcification which is known to be as a multifactorial induced process (Doherty et al., 2004). In fact, miR-301a which is up-regulated at 6 days was shown to regulate inflammatory cytokine expression in macrophages (Huang et al., 2013). In a complementary way, miR-301a was shown to downregulate NF- $\kappa$ B repressing factor (NKrf), leading to the increased activation of NF- $\kappa$ B (Lu et al., 2011) thus increasing other NF- $\kappa$ B dependent factor expression such as interleukin-6 (IL-6)/TNF- $\alpha$  (Karin & Greten, 2005). TNF- $\alpha$  activated NF- $\kappa$ B was shown to promote inflammation-accelerated vascular calcification by inhibiting ankylosis protein homolog expression and consequent pyrophosphate secretion (Zhao et al., 2012). Moreover, MAPK3/ERK1 pathway might be also activated by miR-301a (Cao et al., 2010). In fact, phosphorylated ERK1/2 was shown to be involved in promoting calcification and osteochondrogenic differentiation. ERK1/2 activation decreases myocardin and SMC lineage markers to generate the osteochondrogenic precursor state (Speer et al., 2009) and has an essential role in expression of osteogenic genes including Runx2, osteopontin, osteocalcin, and bone sialoprotein (Xiao et al., 2000). Moreover, ERK1/2 pathway was found to be modulated by and it mediates the action of inorganic phosphate on bone-forming cells (Khoshniat et al., 2011; Spina et al., 2013). Thus, it seems that miR-301a is promoting an inflammatory state which is known to be involved in the calcification process in ESRD patients as evidenced by the strong link between inflammatory cytokines/proteins (e.g., IL-6 and C-reactive protein: CRP) and coronary artery, aortic and valvular calcification (Wang et al., 2008). Another upregulated miR at day 6 is miR-328, whose overexpression was shown to upregulate calcineurin and promote calcineurin-dependent 3 (NFATc3) translocation into the nucleus (Chen, 1988). NFAT signaling pathway was identified as a novel regulator of oxidized low-density lipoprotein (LDL)-induced trans-differentiation of human coronary artery SMCs toward an osteoblast-like phenotype (Goettsch, Rauner, Hamann, et al., 2011). NFATc1 was identified in calcified aortic valves, indicating its involvement in the calcification process (Alexopoulos et al., 2010). Furthermore, the downregulation of miR-409 at day 6 may activate genes that are repressed by this miR like MMP2/9. MMP-2 is constitutively expressed in endothelial cells and VSMCs whereas MMP-9 expression is more common in monocytes and other bone marrow-derived cells (Bäck, Ketelhuth, & Agewall, 2010).

Serum levels of MMP-9 and MMP-2 are elevated in hemodialysis patients with a history of cardiovascular disease compared to those without disease and normal controls (Pawlak, Pawlak, & Mysliwiec, 2007) and blockade of MMP activity can inhibit arterial calcification (Chen et al., 2011). Chung et al. (2009) also showed that diabetic arteries of a different set of patients with CKD demonstrated increased MMP-2 and MMP-9 activities by 42% and 116%, respectively, compared with non-diabetic arteries of patients with CKD. This enhanced MMP expression is highly correlated with arterial stiffness and pulse wave velocity (Chung et al., 2009). Recently, Peiskerová et al. (2009) reported that serum MMP-2 levels are higher in 80 patients with CKD stages 1–5 and 44 healthy control subjects. The occurrence of calcification in tunica media of the radial artery of uremic patients was correlated with the expression of MMP-2 (Shan et al., 2013). It might be also involved in the development of medial layer vascular calcification in uremic rats (Kumata et al., 2011). Both gelatinases provide essential signals for phenotypic VSMC conversion, matrix remodeling and the initiation of vascular calcification (Hecht et al., 2015, p. 9). MMP-2 and 9 were also shown to promote vascular calcification by upregulating bone morphogenetic protein 2 (BMP-2) which induces expression of RUNX2 and msh-homeobox 2 (*Msx-2*), two proteins associated with phenotype transition of VSMCs in vascular calcification (Zhao et al., 2016).

Previous studies have addressed the implication of some microRNAs in vascular calcification. However, these miRNAs were not identified to be differentially regulated in our miRNA profiling. For example, miR-204, -205, -221, and -222 were found to be downregulated during the calcification of smooth muscle cells (Cui et al., 2012; Mackenzie, Staines, Zhu, Genever, & Macrae, 2014; Qiao, Chen, & Zhang, 2014). Among these, miR-204 and -205 inhibited calcification by targeting Runx2, whereas miR-221 and -222 were found to enhance calcification. Also, miR-223 was shown to be upregulated in Pi-treated human vascular smooth muscle cells (Rangrez et al., 2012). The discrepancies between our study and these studies may be due to one of two reasons. First, the time points tested in these studies may not correspond to the time point tested in our study. On the other hand, these studies were done on cells whereas our model was done on tissues, containing smooth muscle cells with their extracellular matrix which can have important effects on the mechanism of calcification. In the aortic extracellular matrix, many factors may affect calcification; importantly, the elastin degradation products that are usually generated during vascular calcification can affect the expression of different genes in the smooth muscle cells by binding to the elastin laminin receptor (Simionescu, Philips, & Vyavahare, 2005).

In conclusion, in this study we report that microRNAs are pivotal mediators which may contribute to high phosphate-induced calcification of VSMCs and phenotypic switching into osteoblast/chondrocyte like cells in rat arteries. The exact roles of these miRs can be further validated through targeted downregulation by specific anti-miRs or overexpression by lentiviral transduction. From a clinical view, understanding the function of those miRs and

their association with the molecular pathogenesis of vascular calcification will provide novel insights into the development of new therapeutic strategies.

## ACKNOWLEDGMENTS

Authors are grateful to the Lebanese University (LU) and the Lebanese National Council for Scientific Research (CNRS-L) for providing PhD scholarships to Maya Fakhry and Najwa Skafi.

## CONFLICTS OF INTEREST

None declared.

## ORCID

Aida Habib  <http://orcid.org/0000-0001-6027-0043>

Hussein Fayyad-Kazan  <http://orcid.org/0000-0002-3465-4630>

## REFERENCES

- Alexopoulos, A., Bravou, V., Peroukides, S., Kaklamanis, L., Varakis, J., Alexopoulos, D., & Papadaki, H. (2010). Bone regulatory factors NFATc1 and Osterix in human calcific aortic valves. *International Journal of Cardiology*, *139*, 142–149.
- Bäck, M., Ketelhuth, D. F. J., & Agewall, S. (2010). Matrix metalloproteinases in atherothrombosis. *Progress in Cardiovascular Diseases*, *52*, 410–428.
- Belz, G. G. (1995). Elastic properties and Windkessel function of the human aorta. *Cardiovascular Drugs and Therapy*, *9*, 73–83.
- Bessueille, L., & Magne, D. (2015). Inflammation: A culprit for vascular calcification in atherosclerosis and diabetes. *Cellular and Molecular Life Sciences*, *72*, 2475–2489.
- Blacher, J., Guerin, A. P., Pannier, B., Marchais, S. J., & London, G. M. (2001). Arterial calcifications, arterial stiffness, and cardiovascular risk in end-stage renal disease. *Hypertension*, *38*, 938–942.
- Cao, G., Huang, B., Liu, Z., Zhang, J., Xu, H., Xia, W., . . . Shao, N. (2010). Intronic miR-301 feedback regulates its host gene, *skaz*, in A549 cells by targeting MEOX2 to affect ERK/CREB pathways. *Biochemical and Biophysical Research Communications*, *396*, 978–982.
- Chen, L.-J., Chuang, L., Huang, Y.-H., Zhou, J., Lim, S. H., Lee, C.-I., . . . Chiu, J.-J. (2015). MicroRNA mediation of endothelial inflammatory response to smooth muscle cells and its inhibition by atheroprotective shear stress. *Circulation Research*, *116*, 1157–1169.
- Chen, N. X., Duan, D., O'Neill, K. D., Wolisi, G. O., Koczman, J. J., Laclair, R., & Moe, S. M. (2006). The mechanisms of uremic serum-induced expression of bone matrix proteins in bovine vascular smooth muscle cells. *Kidney International*, *70*, 1046–1053.
- Chen, N. X., O'Neill, K. D., Chen, X., Kiattisunthorn, K., Gattone, V. H., & Moe, S. M. (2011). Activation of arterial matrix metalloproteinases leads to vascular calcification in chronic kidney disease. *American Journal of Nephrology*, *34*, 211–219.
- Chen, R. H. (1988). TLC identification of organochlorine (BHC, DDT) pesticide residues in crude drugs. *Zhong Yao Tong Bao Beijing China*, *13*, 34–36.
- Chung, A. W. Y., Yang, H. H. C., Sigrist, M. K., Brin, G., Chum, E., Gourlay, W. A., & Levin, A. (2009). Matrix metalloproteinase-2 and -9 exacerbate arterial stiffening and angiogenesis in diabetes and chronic kidney disease. *Cardiovascular Research*, *84*, 494–504.

- Cui, R.-R., Li, S.-J., Liu, L.-J., Yi, L., Liang, Q.-H., Zhu, X., ... Liao, E.-Y. (2012). MicroRNA-204 regulates vascular smooth muscle cell calcification in vitro and in vivo. *Cardiovascular Research*, 96, 320–329.
- Demer, L. L., & Tintut, Y. (2008). Vascular calcification: Pathobiology of a multifaceted disease. *Circulation*, 117, 2938–2948.
- De Oliveira, R. B., Okazaki, H., Stingham, A. E. M., Drüeke, T. B., Massy, Z. A., & Jorgetti, V. (2013). Vascular calcification in chronic kidney disease: A review. *J. The Jornal Brasileiro de Nefrologia*, 35, 147–161.
- Ding, J., Ghali, O., Lencel, P., Broux, O., Chauveau, C., Devedjian, J. C., ... Magne, D. (2009). TNF-alpha and IL-1beta inhibit RUNX2 and collagen expression but increase alkaline phosphatase activity and mineralization in human mesenchymal stem cells. *Life Sciences*, 84, 499–504.
- Doherty, T. M., Fitzpatrick, L. A., Inoue, D., Qiao, J.-H., Fishbein, M. C., Detrano, R. C., ... Rajavashisth, T. B. (2004). Molecular, endocrine, and genetic mechanisms of arterial calcification. *Endocrine Reviews*, 25, 629–672.
- Erson, A. E., & Petty, E. M. (2008). MicroRNAs in development and disease. *Clinical Genetics*, 74, 296–306.
- Fakhry, M., Hamade, E., Badran, B., Buchet, R., & Magne, D. (2013). Molecular mechanisms of mesenchymal stem cell differentiation towards osteoblasts. *World Journal of Stem Cells*, 5, 136–148.
- Foley, R. N., Parfrey, P. S., & Sarnak, M. J. (1998a). Clinical epidemiology of cardiovascular disease in chronic renal disease. *American Journal of Kidney Diseases*, 32, S112–S119.
- Foley, R. N., Parfrey, P. S., & Sarnak, M. J. (1998b). Epidemiology of cardiovascular disease in chronic renal disease. *Journal of the American Society of Nephrology*, 9, S16–S23.
- Gámez, B., Rodríguez-Carballo, E., Bartrons, R., Rosa, J. L., & Ventura, F. (2013). MicroRNA-322 (miR-322) and its target protein Tob2 modulate Osterix (Osx) mRNA stability. *The Journal of Biological Chemistry*, 288, 14264–14275.
- Gansevoort, R. T., Matsushita, K., van der Velde, M., Astor, B. C., Woodward, M., Levey, A. S., ... Chronic Kidney Disease Prognosis Consortium. (2011). Lower estimated GFR and higher albuminuria are associated with adverse kidney outcomes. A collaborative meta-analysis of general and high-risk population cohorts. *Kidney International*, 80, 93–104.
- Giachelli, C. M. (2009). The emerging role of phosphate in vascular calcification. *Kidney International*, 75, 890–897.
- Goettsch, C., Rauner, M., Hamann, C., Sinnigen, K., Hempel, U., Bornstein, S. R., & Hofbauer, L. C. (2011). Nuclear factor of activated T cells mediates oxidised LDL-induced calcification of vascular smooth muscle cells. *Diabetologia*, 54, 2690–2701.
- Goettsch, C., Rauner, M., Pacyna, N., Hempel, U., Bornstein, S. R., & Hofbauer, L. C. (2011). MiR-125b regulates calcification of vascular smooth muscle cells. *American Journal of Pathology*, 179, 1594–1600.
- Goodman, W. G., Goldin, J., Kuizon, B. D., Yoon, C., Gales, B., Sider, D., ... Salusky, I. B. (2000). Coronary-artery calcification in young adults with end-stage renal disease who are undergoing dialysis. *The New England Journal of Medicine*, 342, 1478–1483.
- Gross, P., Six, I., Kamel, S., & Massy, Z. A. (2014). Vascular toxicity of phosphate in chronic kidney disease: Beyond vascular calcification. *Circulation Journal—Official Journal of the Japanese Circulation Society*, 78, 2339–2346.
- Guo, H., Ingolia, N. T., Weissman, J. S., & Bartel, D. P. (2010). Mammalian microRNAs predominantly act to decrease target mRNA levels. *Nature*, 466, 835–840.
- Hecht, E., Freise, C., Websky, K. V., Nasser, H., Kretschmar, N., Stawowy, P., ... Querfeld, U. (2015). The matrix metalloproteinases 2 and 9 initiate uraemic vascular calcifications. *Nephrology Dialysis Transplantation*, 31, 789–797.
- Hong, L., Sharp, T., Khorsand, B., Fischer, C., Eliason, S., Salem, A., ... Amendt, B. A. (2016). MicroRNA-200c represses IL-6, IL-8, and CCL5 expression and enhances osteogenic differentiation. *PLoS ONE*, 11, e0160915.
- Huang, L., Liu, Y., Wang, L., Chen, R., Ge, W., Lin, Z., ... Jiang, M. (2013). Down-regulation of miR-301a suppresses pro-inflammatory cytokines in Toll-like receptor-triggered macrophages. *Immunology*, 140, 314–322.
- Huntzinger, E., & Izaurralde, E. (2011). Gene silencing by microRNAs: Contributions of translational repression and mRNA decay. *Nature Reviews Genetics*, 12, 99–110.
- Hu, R., Li, H., Liu, W., Yang, L., Tan, Y.-F., & Luo, X.-H. (2010). Targeting miRNAs in osteoblast differentiation and bone formation. *Expert Opinion on Therapeutic Targets*, 14, 1109–1120.
- Jansen, R. S., Duijst, S., Mahakena, S., Sommer, D., Szeri, F., Váradi, A., ... van de Wetering, K. (2014). ABCG6-mediated ATP secretion by the liver is the main source of the mineralization inhibitor inorganic pyrophosphate in the systemic circulation—brief report. *Arteriosclerosis, Thrombosis, and Vascular Biology*, 34, 1985–1989.
- Jono, S., McKee, M. D., Murry, C. E., Shioi, A., Nishizawa, Y., Mori, K., ... Giachelli, C. M. (2000). Phosphate regulation of vascular smooth muscle cell calcification. *Circulation Research*, 87, E10–E17.
- Karin, M., & Greten, F. R. (2005). NF-kappaB: Linking inflammation and immunity to cancer development and progression. *Nature Reviews Immunology*, 5, 749–759.
- Khoshniat, S., Bourguine, A., Julien, M., Petit, M., Pilet, P., Rouillon, T., ... Beck, L. (2011). Phosphate-dependent stimulation of MGP and OPN expression in osteoblasts via the ERK1/2 pathway is modulated by calcium. *Bone*, 48, 894–902.
- Kumata, C., Mizobuchi, M., Ogata, H., Koiwa, F., Kondo, F., Kinugasa, E., & Akizawa, T. (2011). Involvement of matrix metalloproteinase-2 in the development of medial layer vascular calcification in uremic rats. *Therapeutic Apheresis and Dialysis*, 15(Suppl 1), 18–22.
- Larsson, T. E., Olsson, H., Hagström, E., Ingelsson, E., Arnlöv, J., Lind, L., & Sundström, J. (2010). Conjoint effects of serum calcium and phosphate on risk of total, cardiovascular, and noncardiovascular mortality in the community. *Arteriosclerosis, Thrombosis, and Vascular Biology*, 30, 333–339.
- Lencel, P., Delplace, S., Pilet, P., Leterme, D., Miellot, F., Sourice, S., ... Magne, D. (2011). Cell-specific effects of TNF- $\alpha$  and IL-1 $\beta$  on alkaline phosphatase: Implication for syndesmophyte formation and vascular calcification. *Laboratory Investigation*, 91, 1434–1442.
- Leopold, J. A. (2014). MicroRNAs regulate vascular medial calcification. *Cells*, 3, 963–980.
- Lewis, R. (2012). Mineral and bone disorders in chronic kidney disease: New insights into mechanism and management. *Annals of Clinical Biochemistry*, 49, 432–440.
- Lomashvili, K. A., Cobbs, S., Hennigar, R. A., Hardcastle, K. I., & O'Neill, W. C. (2004). Phosphate-induced vascular calcification: Role of pyrophosphate and osteopontin. *Journal of the American Society of Nephrology*, 15, 1392–1401.
- Lomashvili, K. A., Garg, P., Narisawa, S., Millan, J. L., & O'Neill, W. C. (2008). Upregulation of alkaline phosphatase and pyrophosphate hydrolysis: Potential mechanism for uremic vascular calcification. *Kidney International*, 73, 1024–1030.
- London, G. M., Guérin, A. P., Marchais, S. J., Métivier, F., Pannier, B., & Adda, H. (2003). Arterial media calcification in end-stage renal disease: Impact on all-cause and cardiovascular mortality. *Nephrology Dialysis Transplantation*, 18, 1731–1740.
- Lu, Z., Li, Y., Takwi, A., Li, B., Zhang, J., Conklin, D. J., ... Li, Y. (2011). MiR-301a as an NF- $\kappa$ B activator in pancreatic cancer cells. *EMBO Journal*, 30, 57–67.
- Mackenzie, N. C. W., Staines, K. A., Zhu, D., Genever, P., & Macrae, V. E. (2014). MiRNA-221 and miRNA-222 synergistically function to promote vascular calcification. *Cell Biochemistry and Function*, 32, 209–216.
- Masuda, M., Miyazaki-Anzai, S., Levi, M., Ting, T. C., & Miyazaki, M. (2013). PERK-eIF2 $\alpha$ -ATF4-CHOP signaling contributes to TNF $\alpha$ -induced

- vascular calcification. *Journal of the American Heart Association*, 2, e000238.
- Narisawa, S., Harmey, D., Yadav, M. C., O'Neill, W. C., Hoylaerts, M. F., & Millán, J. L. (2007). Novel inhibitors of alkaline phosphatase suppress vascular smooth muscle cell calcification. *Journal of Bone and Mineral Research*, 22, 1700–1710.
- Nitschke, Y., & Rutsch, F. (2012). Genetics in arterial calcification: Lessons learned from rare diseases. *Trends in Cardiovascular Medicine*, 22, 145–149.
- Panizo, S., Naves-Díaz, M., Carrillo-López, N., Martínez-Arias, L., Fernández-Martín, J. L., Ruiz-Torres, M. P., ... Rodríguez, I. (2015). MicroRNAs 29b, 133b, and 211 regulate vascular smooth muscle calcification mediated by high phosphorus. *Journal of the American Society of Nephrology*.
- Pawlak, K., Pawlak, D., & Mysliwiec, M. (2007). Serum matrix metalloproteinase-2 and increased oxidative stress are associated with carotid atherosclerosis in hemodialyzed patients. *Atherosclerosis*, 190, 199–204.
- Peiskerová, M., Kalousová, M., Kratochvílová, M., Dusilová-Sulková, S., Uhrová, J., Bandúr, S., ... Tesar, V. (2009). Fibroblast growth factor 23 and matrix-metalloproteinases in patients with chronic kidney disease: Are they associated with cardiovascular disease? *Kidney Blood Pressure Research*, 32, 276–283.
- Qiao, W., Chen, L., & Zhang, M. (2014). MicroRNA-205 regulates the calcification and osteoblastic differentiation of vascular smooth muscle cells. *Cellular Physiology and Biochemistry*, 33, 1945–1953.
- Rana, T. M. (2007). Illuminating the silence: Understanding the structure and function of small RNAs. *Nature Reviews Molecular Cell Biology*, 8, 23–36.
- Rangrez, A. Y., M'Baya-Moutoula, E., Metzinger-Le Meuth, V., Hénaut, L., Djelouat, M. S. E. I., Benchitrit, J., ... Metzinger, L. (2012). Inorganic phosphate accelerates the migration of vascular smooth muscle cells: Evidence for the involvement of miR-223. *PLoS ONE*, 7, e47807.
- Reddy, M. A., Jin, W., Villeneuve, L., Wang, M., Lanting, L., Todorov, I., ... Natarajan, R. (2012). Pro-inflammatory role of microRNA-200 in vascular smooth muscle cells from diabetic mice. *Arteriosclerosis, Thrombosis, and Vascular Biology*, 32, 721–729.
- Rutsch, F., Vaingankar, S., Johnson, K., Goldfine, I., Maddux, B., Schauerte, P., ... Terkeltaub, R. (2001). PC-1 nucleoside triphosphate pyrophosphohydrolase deficiency in idiopathic infantile arterial calcification. *American Journal of Pathology*, 158, 543–554.
- Sage, A. P., Tintut, Y., & Demer, L. L. (2010). Regulatory mechanisms in vascular calcification. *Nature Reviews Cardiology*, 7, 528–536.
- Schlieper, G., Krüger, T., Djuric, Z., Damjanovic, T., Markovic, N., Schurgers, L. J., ... Dimkovic, N. (2008). Vascular access calcification predicts mortality in hemodialysis patients. *Kidney International*, 74, 1582–1587.
- Shan, A., Zhou, C., He, Y., Feng, W., Chen, G., & Zhong, G. (2013). Expression of both matrix metalloproteinase-2 and its tissue inhibitor-2 in tunica media of radial artery in uremic patients. *Renal Failure*, 35, 37–42.
- Sheen, C. R., Kuss, P., Narisawa, S., Yadav, M. C., Nigro, J., Wang, W., ... Millán, J. L. (2015). Pathophysiological role of vascular smooth muscle alkaline phosphatase in medial artery calcification. *Journal of Bone and Mineral Research*, 30, 824–836.
- Sigrist, M. K., Taal, M. W., Bungay, P., & McIntyre, C. W. (2007). Progressive vascular calcification over 2 years is associated with arterial stiffening and increased mortality in patients with stages 4 and 5 chronic kidney disease. *Clinical Journal of the American Society of Nephrology*, 2, 1241–1248.
- Simionescu, A., Philips, K., & Vyavahare, N. (2005). Elastin-derived peptides and TGF-beta1 induce osteogenic responses in smooth muscle cells. *Biochemical and Biophysical Research Communications*, 334, 524–532.
- Song, L., Li, D., Li, X., Ma, L., Bai, X., Wen, Z., ... Peng, L. (2017). Exposure to PM2.5 induces aberrant activation of NF-κB in human airway epithelial cells by downregulating miR-331 expression. *Environmental Toxicology and Pharmacology*, 50, 192–199.
- Speer, M. Y., Yang, H.-Y., Brabb, T., Leaf, E., Look, A., Lin, W.-L., ... Giachelli, C. M. (2009). Smooth muscle cells give rise to osteochondrogenic precursors and chondrocytes in calcifying arteries. *Circulation Research*, 104, 733–741.
- Spina, A., Sorvillo, L., Di Maiolo, F., Esposito, A., D'Auria, R., Di Gesto, D., ... Naviglio, S. (2013). Inorganic phosphate enhances sensitivity of human osteosarcoma U2OS cells to doxorubicin via a p53-dependent pathway. *Journal of Cellular Physiology*, 228, 198–206.
- Stenvinkel, P. (2010). Chronic kidney disease: A public health priority and harbinger of premature cardiovascular disease. *Journal of Internal Medicine*, 268, 456–467.
- Tintut, Y., Patel, J., Parhami, F., & Demer, L. L. (2000). Tumor necrosis factor-α promotes in vitro calcification of vascular cells via the cAMP pathway. *Circulation*, 102, 2636–2642.
- Vattikuti, R., & Towler, D. A. (2004). Osteogenic regulation of vascular calcification: An early perspective. *American Journal of Physiology Endocrinology and Metabolism*, 286, E686–E696.
- Wang, A. Y.-M., Lam, C. W.-K., Wang, M., Chan, I. H.-S., Yu, C.-M., Lui, S.-F., & Sanderson, J. E. (2008). Increased circulating inflammatory proteins predict a worse prognosis with valvular calcification in end-stage renal disease: A prospective cohort study. *American Journal of Nephrology*, 28, 647–653.
- Xiao, G., Jiang, D., Thomas, P., Benson, M. D., Guan, K., Karsenty, G., & Franceschi, R. T. (2000). MAPK pathways activate and phosphorylate the osteoblast-specific transcription factor, Cbfa1. *The Journal of Biological Chemistry*, 275, 4453–4459.
- Yang, Z., Zheng, B., Zhang, Y., He, M., Zhang, X., Ma, D., ... Wen, J. (2015). MiR-155-dependent regulation of mammalian sterile 20-like kinase 2 (MST2) coordinates inflammation, oxidative stress and proliferation in vascular smooth muscle cells. *Biochimica et Biophysica Acta*, 1852, 1477–1489.
- Zhao, G., Xu, M.-J., Zhao, M.-M., Dai, X.-Y., Kong, W., Wilson, G. M., ... Wang, X. (2012). Activation of nuclear factor-kappa B accelerates vascular calcification by inhibiting ankylosis protein homolog expression. *Kidney International*, 82, 34–44.
- Zhao, Y.-G., Meng, F.-X., Li, B.-W., Sheng, Y.-M., Liu, M.-M., Wang, B., ... Xiu, R.-J. (2016). Gelatinases promote calcification of vascular smooth muscle cells by up-regulating bone morphogenetic protein-2. *Biochemical and Biophysical Research Communications*, 470, 287–293.
- Zhu, D., Mackenzie, N. C. W., Farquharson, C., & Macrae, V. E. (2012). Mechanisms and clinical consequences of vascular calcification. *Frontiers in Endocrinology*, 3, 95.

**How to cite this article:** Fakhry M, Skafi N, Fayyad-Kazan M, et al. Characterization and assessment of potential microRNAs involved in phosphate-induced aortic calcification. *J Cell Physiol*. 2018;233:4056–4067. <https://doi.org/10.1002/jcp.26121>